

A Small Model Fixed Field Alternating Gradient Radial Sector Accelerator

#102

Lawrence W. Jones and Kent M. Terwilliger  
University of Michigan and Midwestern Universities  
Research Association.\* April 3, 1956

104

### I. Introduction

An eight sector fixed field alternating gradient electron betatron model of the radial sector type has been constructed and operated successfully. The design, construction, and operation of this model have been carried out at the University of Michigan. Very important contributions were made by Professor F. T. Cole, Professor D. W. Kerst, Professor R. O. Haxby, and Dr. C. H. Pruett. The following discussion summarizes the design, construction, sigma testing, and accelerated beam of the model.

### II. General Description

Early in 1955, after the principles of fixed field alternating gradient accelerators had been developed, it was decided to study the operation of an F.F.A.G. system with a small electron betatron. Since the radial sector type was more completely understood theoretically then, the first model was of that type. Subsequently, a second model of the spiral sector type was begun and is still under construction at the University of Illinois. Betatron acceleration of electrons is used, since the emphasis of studies with this model was to be on orbits and betatron oscillations, and the betatron accelerating system was simpler to assemble and operate than a frequency modulated R. F. system. The overall scale was chosen large enough to give adequate access to all components, and yet small enough so that parts would be easy to construct and handle and magnetic

\* Assisted by the National Science Foundation and the Office of Naval Research.

## **DISCLAIMER**

**This report was prepared as an account of work sponsored by an agency of the United States Government. Neither the United States Government nor any agency thereof, nor any of their employees, makes any warranty, express or implied, or assumes any legal liability or responsibility for the accuracy, completeness, or usefulness of any information, apparatus, product, or process disclosed, or represents that its use would not infringe privately owned rights. Reference herein to any specific commercial product, process, or service by trade name, trademark, manufacturer, or otherwise does not necessarily constitute or imply its endorsement, recommendation, or favoring by the United States Government or any agency thereof. The views and opinions of authors expressed herein do not necessarily state or reflect those of the United States Government or any agency thereof.**

---

## **DISCLAIMER**

**Portions of this document may be illegible in electronic image products. Images are produced from the best available original document.**

fields would not be too low. The resulting accelerator injects electrons of from 20 to 30 kilovolts at a radius of 34 cm. and accelerates them in magnetic fields of from 40 to 150 gauss to an energy of about 400 kilovolts at a radius of 50 centimeters. There are sixteen magnets ( $N = 8$ ) with the field alternating direction in successive magnets. Although more sectors would have allowed a smaller radial aperture and larger  $\nu$  values (the number of betatron oscillations per revolution), it would also have required a smaller vertical aperture and would have otherwise complicated construction.

A summary of the design parameters is included below.

$N = 8$ , the number of magnet pairs (sectors.)

$R_1/\rho = 2.85$  } the ratio of the orbit radius to the  
 $R_2/\rho = 2.59$  } radius of curvature at the centers of positive curvature and negative curvature magnets.

$n_1 = \frac{R}{H} \frac{dH}{dr} = 1.18$ , at the center of a positive curvature magnet.

$k = \frac{R}{H} \frac{dH}{dr} = 3.36$ , at every point in the machine

$\Theta_1 = 25^\circ 42'$ , the angle subtended by positive curvature magnets.

$\Theta_2 = 10^\circ 26'$ , the angle subtended by negative curvature magnets.

$\Theta_s = 4^\circ 26'$ , the angle subtended by "straight" sections.

$R_i = 32$  cm. the inner and outer radii of the inside of the vacuum tank.

$R_o = 54$  cm. }

$G_1 = 4.0$  cm. the magnet gap at 32 cm. radius.

$G/R = \text{constant}$ , for all  $R$  across the useful aperture.

$Z = 2.41$  cm., the total vertical aperture available inside the vacuum tank.

$$\left. \begin{array}{l} \sigma_x = 126^\circ \\ \sigma_z = 81^\circ \\ \nu_x = 2.80 \\ \nu_z = 1.81 \end{array} \right\}$$

the radial and vertical betatron phase shift per sector.

the radial and vertical numbers of betatron oscillations per revolution.

### III. Design Calculations

A first approximation to the  $\sigma$  or  $\nu$  values resulting from the design can be obtained assuming the particle equilibrium orbits follow along lines of constant field within the geometrical boundaries of the magnets, then along straight lines in the "straight" sections between magnets, assumed field free in this approximation. The effect of magnet edges can be represented by thin magnetic lenses of focal length proportional to the tangent of the angle,  $\phi$ , between the equilibrium orbit and the normal to the magnet edge. The cosines of the betatron oscillation phase per sector,  $\sigma$ , can then be obtained as products of simple matrices. When fields in the positive curvature magnets have the same value on an equilibrium orbit as those in the negative curvature magnets, and if the variations of  $n$  within sectors is neglected, the expressions for  $\sigma_x$  and  $\sigma_z$  using this "hard edge" approximation take on the form below.

MARK Ib Cos σ Expressions :

$$\begin{aligned}\cos \sigma_x &= \cos \phi_1 \cosh \phi_2 [1 + 4t\delta + 2t^2\delta^2] \\ &+ \sin \phi_1 \sinh \phi_2 \left[ \left( \frac{\kappa_2}{\kappa_1} - \frac{\kappa_1}{\kappa_2} \right) \frac{(1+t\delta)^2}{2} + \frac{(2t+t^2\delta)^2}{2\kappa_1\kappa_2} - \frac{\kappa_1\kappa_2\delta^2}{2} \right] \\ &+ \sin \phi_1 \cosh \phi_2 (1+t\delta) \left[ \frac{2t+t^2\delta}{\kappa_1} - \kappa_1\delta \right] \\ &+ \cos \phi_1 \sinh \phi_2 (1+t\delta) \left[ \frac{2t+t^2\delta}{\kappa_2} + \kappa_2\delta \right]\end{aligned}$$

$$\begin{aligned}\cos \sigma_y &= \cos \psi_2 \cosh \psi_1 [1 - 4t\delta + 2t^2\delta^2] \\ &+ \sin \psi_2 \sinh \psi_1 \left[ \frac{(-2t+t^2\delta)^2}{2\kappa^2} + \frac{\kappa^2\delta^2}{2} \right] \\ &+ \sin \psi_2 \cosh \psi_1 \left[ \frac{-2t+t^2\delta}{\kappa} - \kappa\delta \right] (1-t\delta) \\ &+ \cos \psi_2 \sinh \psi_1 \left[ \frac{-2t+t^2\delta}{\kappa} + \kappa\delta \right] (1-t\delta)\end{aligned}$$

$$t = \tan \phi$$

$$\phi_1 = \kappa_1 \frac{s_1}{\rho}$$

$$\delta = \frac{l}{\rho}$$

$$\phi_2 = \kappa_2 \frac{s_2}{\rho}$$

$$\kappa = \sqrt{n}$$

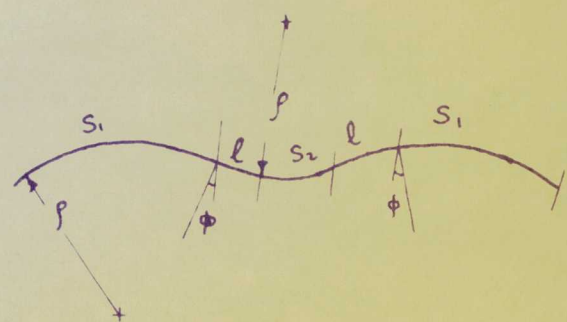
$$\psi_1 = \kappa \frac{s_1}{\rho}$$

$$\kappa_1 = \sqrt{n+1}$$

$$\psi_2 = \kappa \frac{s_2}{\rho}$$

$$\kappa_2 = \sqrt{n-1}$$

$$n = \left| \frac{\rho}{H} \frac{dH}{dr} \right|$$



The effect of magnet edges in this model is to provide vertical focussing and radial defocussing. Since this is also the function of the negative curvature magnets, these magnets may be made shorter, hence the "circumference factor" (ratio between the mean equilibrium orbit radius and radius of curvature) is reduced over what it would be when no magnet edge effects are considered. This edge focussing is more important as the number of sectors is reduced, so that stability may be achieved in designs of four sectors when no negative curvature magnets are present (e.g. the Thomas Cyclotron).

More accurate calculations of  $\sigma$  were made by Cole and Kerst including the fringing fields at the edges of magnets by representing the fields in the machine as  $H(x) F(s)$ , where  $s$  is the arc length along an equilibrium orbit and  $x$  is the displacement perpendicular to that orbit. In the original design, values of  $F(s)$  were deduced by combining conformal mapping solutions of simple geometries. In this calculation, the variation of the field index,  $n$ , within magnets due to the "scalloping" of the equilibrium orbits was also included. The equilibrium orbits vary in radius from the center of the machine by 10% between the centers of positive curvature magnets and negative curvature magnets (see figure 1.)

It was felt desirable to have all pertinent magnet dimensions "scale", that is, to have dimensions such as straight section length and magnet aperture proportional to the machine radius. Equilibrium orbits then differ from each other only by a scale factor, and  $\sigma_x$  and  $\sigma_z$  should be independent of radius.

After the magnets were built, the measured magnetic fields were used to compute equilibrium orbits and to calculate the  $\sigma_s$ .

Non-linear effects were not included in any of these calculations.

#### IV. Magnets

The magnets for this model were designed by, and their construction and field testing supervised by R. O. Haxby. Photographs and drawings of the magnets are shown in figures 2 and 3. To preserve scaling, the magnet aperture increases with radius and the required field gradient is then produced by distributed pole-face windings. The magnets are made of 10-05 low carbon steel one and one eighth inch thick. Pole face windings were made by first machining grooves on a block of lucite, then winding enameled copper wire into the grooves. A coating of cold-setting araldite was then spread over the wires and a sheet of thin aluminum placed on that. After the plastic had set, the lucite block was removed and the aluminum sheet with the coils cemented to it could be bolted to the iron. Several identical coils could thus be made from one lucite block.

The field gradients were checked using a flip coil system and a flux meter. Three coils were mounted on one shaft, the two outer ones to measure gradient and the center one to measure the field. In general the fluxmeter was used in a bridge circuit as a null detector, so that  $\frac{1}{H} \frac{dH}{dr}$  could be derived from resistor values alone. It was observed that when measurements

were made on a magnet separated from others, the results were significantly different even at the center of the gap in the low field region from measurements made when several magnets were adjacent to each other. This is probably due to the variation of permeability of the magnet return yokes with flux density. The field gradient can be adjusted by adding currents through a ten turn coil around the back leg of each magnet. All magnets were corrected to give  $k$  and  $H$  at the injection radius within  $\pm 1\%$  of the mean values.

#### V. Accelerator Construction

The accelerator was built on a one and one quarter inch cast aluminum plate supported at three points by aluminum "legs". This table is cut at two azimuths and cemented to an insulating sheet with thermo-setting plastic to avoid short circuiting the betatron accelerating core. Holes are jig-bored through the table and dowel pins through those holes into matching holes in the magnets, position all magnets to within 0.001 inches. The table is level to within 0.003 inches. The vacuum tank is made of welded aluminum, and is in two halves, bolted together with insulating gaskets again to avoid short circuiting the betatron. Access ports are provided at the centers of magnets around the inside of the tank, and between every pair of magnets around the outside of the tank.

The betatron core is excited sinusoidally by a 500 cycle alternating current generator to provide approximately 40 volts per turn maximum to the electrons. Its 500 pounds of 0.014 inch transformer iron driven to  $\pm 10,000$  gauss dissipate 6

kilowatts of heat at full excitation, and water cooling of the laminations is provided. The field magnets are excited with all positive curvature magnets in one series circuit and all negative curvature magnets in another. For injection a standard betatron electron gun is used. It may either be used with a pulse transformer to give a one microsecond pulse at 500 milliamperes peak emission every betatron cycle, or with a D.C. power supply to give 3 milliamperes emission continuously.

Photographs of the assembled accelerator are included in figures 4 and 5.

#### VI. Static $\sigma$ Tests

Tests of the betatron oscillation  $\sigma$ 's were made by using a special injector which produced a direct current beam of electrons through a one millimeter hole in its anode, the injector being placed at the center of a positive curvature magnet. At the center of the next positive magnet, a metal plate with several small holes in it was placed to define rays of electrons. These then produced bright spots on a zinc sulphide fluorescent screen onto which a one millimeter grid had been ruled placed at the center of the next positive magnet. These spots could then be observed visually through a lucite port in the vacuum tank and their separations determined. From Floquet's theorem for linear oscillations, the value of cosine  $\sigma_x$  can be deduced from the ratio of the separation of two radial image points,  $\Delta x_2$ , to the radial separation of two holes in the metal plate,  $\Delta x_1$ , and similarly for cosine  $\sigma_z$ ; thus:

$$\cos \sigma_x = \frac{1}{2} \left( \frac{\Delta x_2}{\Delta x_1} \right)$$

$$\cos \sigma_z = \frac{1}{2} \left( \frac{\Delta z_2}{\Delta z_1} \right).$$

The geometry used in these tests is represented schematically in figure 6.

By placing the fluorescent screen at the center of the positive magnet just before the injector, the electrons travel seven-eighths of one revolution before being imaged. Then:

$$\frac{\Delta x_7}{\Delta x_1} = \frac{\sin 7 \sigma_x}{\sin \sigma_x}$$

$$\frac{\Delta z_7}{\Delta z_1} = \frac{\sin 7 \sigma_z}{\sin \sigma_z}$$

It was clearly evident from the seven sector sigma tests that nonlinearities are important.

The values of  $\sigma$  can be varied in either of two ways. First, by changing the ratio of currents through the positive and negative magnets the equilibrium orbit scalloping is altered and  $\sigma_z$  is strongly affected. This method of tuning preserves scaling, i.e. the geometrical similarity of orbits at all radii. Second, by changing the falloff index,  $k$ , in all magnets,  $\sigma_x$  is strongly affected while there is almost no effect on  $\sigma_z$ . Although in principle, scaling would be preserved by changing  $k$ , in practice  $k$  is altered by exciting a ten turn winding around the magnet return yokes. This produces a change of  $k$  which is maximum at the injector radius, and only 40% of that maximum at the target radius.

The dependence of the  $\sigma$ 's on changing  $k$  was found from the two sector test. The seven sector tests were made tuning only

with the current ratios, leaving  $k$  at the design value.

The values of  $\sigma$  were deduced in the presence of non-linearities in the seven sector tests by tuning for nodes of the oscillations, e.g. finding values of tuning which brought rays from the injector again to a focus at the fluorescent screen. Vertically, two nodes were observed for different current ratios, and a linear interpolation between them agreed with the values of  $\sigma_z$  obtained from image dot spacings at intermediate tunings. Radially, nodes were observed over a range of tunings, each node occurring at a different radial amplitude. From this data, the current ratios corresponding to a half-integral number of radial oscillations in seven sectors for a range of amplitudes was found, the amplitude of oscillation corresponding to half the radial separation between the injector and the focal point on the screen. The values obtained are shown in figure 7 together with the other  $\sigma$  test results. The dependence of  $\sigma_x$  for a given amplitude on tuning was found using the linear theory and the spacings of one pair of rays. The assumption was then made that the variation of  $\sigma_x$  with amplitude was constant over the range of tuning of interest, so that by extending parallel lines through the nodal points,  $\sigma_x$  for any tuning and any radial amplitude may be deduced. As a result, we conclude that  $\sigma_x$  decreases with amplitude by 6% in going from almost zero amplitude to 2.2 cm. amplitude at the center of positive magnets.

For the design values of  $k$  (3.36) and current ratio (1.00), the data give  $\sigma_x = 2.87$  and  $\sigma_z = 2.12$  for small amplitude

oscillations. The theory gives  $\nu_x = 2.70$  and  $\nu_z = 1.90$  using the measured magnetic fields. This discrepancy is not yet well understood.

### VII. Accelerated Beam

Using a standard pulsed betatron injector, a search was made for accelerated beam. Since the peak accelerating voltage expands the equilibrium orbit by only about 0.008 cm. per revolution at injection, and the injector anode extends beyond the filament 0.2 cm., an expander pulse was supplied to accelerate the electrons with 500 volts per turn for several turns at injection. The expander pulse was provided by discharging a condenser across the vacuum tank through a type 5C22 hydrogen thyratron. The vacuum tank appears in this circuit as a one microhenry inductance, and the resulting voltage pulse is half a cosine curve with a frequency of 1.6 megacycles per second. Injection is then triggered on the second part of this curve.

With the expander operating, accelerated beam was observed for several different tuning conditions. Either the x-rays from a target probe struck by the electrons could be observed with a scintillation counter, or the current pulse of electrons on the target probe could be observed directly. The energy of the accelerated electrons may be deduced both from the time delay of the beam pulse from injection and from the radial position of the target probe. Figure 8 shows the electron energy and the magnetic field as a function of radius for typical operating conditions.

With the target probe moved in to within six centimeters of the injector radius, a systematic search was made over the ranges of  $k$  tuning and current ratio tuning available for accelerated beam. Since this beam has been accelerated for about 40 microseconds, it has circulated in the machine for about 2000 revolutions. The graph presented in figure 9 summarizes the regions where beam was found in this test, the values of  $\nu$  being deduced from the  $\sigma$  testing data described above. This smaller radial aperture was used to minimize the effects of the radial variation of  $k$  when  $k$  tuning was used. The regions indicated on the graph where beam was found are located assuming small radial oscillation amplitudes. Larger amplitudes up to two centimeters would reduce the indicated values of  $\nu_x$  by about 0.17.

Full energy accelerated beam has been observed in each of the three regions indicated for the 40 microsecond beam. When brought to full energy, the beam reaches the probe in 160 microseconds. By reducing the betatron core excitation the beam can be made to last 430 microseconds. Although this is probably not a maximum, it corresponds to over 20,000 revolutions.

The beam intensity, as determined by the current on the probe, corresponds to  $2 \times 10^7$  electrons per pulse accelerated to full energy. This represents a minimum figure, since no account is taken of scattering and secondary emission from the target. The operating pressure in the tank is  $10^{-5}$  mm Hg, and it is observed that increasing it to  $1.5 \times 10^{-5}$  mm Hg decreases the beam by a factor of two.

In the centers of the two large regions of the  $\mathcal{V}_x$ ,  $\mathcal{V}_z$  plane where beam was found, it was observed that the expander pulse could be turned off and considerable beam remained, providing the injector voltage was increased by 10% to 15%. This corresponds to using larger radial oscillation amplitudes.

### VIII. Continuous Beam

Although the major purpose of this machine is to study the application of the F.F.A.G. principle to very high energy accelerators, an interesting application of F.F.A.G. is in high intensity electron betatrons of medium energy using continuous injection. To examine this possibility, the injector of the model was connected to a D.C. supply and operated at 3 milliamperes emission. Accelerated beam was observed for the same general tuning conditions as those for which pulsed beam had been found, however in this case the beam appeared over a full 600 microseconds and repeated every two milliseconds. Tuning conditions were, however, far more critical than with pulsed injection using the expander. For optimum conditions, the electron current on the target probe was  $1.5 \times 10^{-8}$  amperes time average, or about  $10^8$  electrons per pulse. Although again these represent minimum values, the capture efficiency from this gun into useful orbits is extremely low compared to operation using the expander. An injection system specifically designed for D.C. operation may be tried later in an attempt to improve this efficiency.

## IX. Future Program

In order to measure the values of  $\mathcal{V}$  (or  $\sigma$ ) in the accelerated beam, a method employed successfully with the Michigan synchrotron is being used. This consists of exciting a pair of probe paddles with a radio frequency voltage of from 100 to 300 volts. When the applied frequency is equal to the frequency of revolution times the difference between an integer and  $\mathcal{V}$ , the amplitude of oscillation will grow linearly until the beam is destroyed. Two frequencies should be effective; one corresponding to an integer minus  $\mathcal{V}$ , the other corresponding to  $\mathcal{V}$  minus the next smaller integer. If both frequencies are observed, the frequency of particle revolution may be found as the sum of the two. When the two paddles are excited in parallel, the R.F. field is mostly radial, and  $\mathcal{V}_x$  may be determined. When the R.F. is applied between the two paddles, vertical oscillations will be most strongly driven, and  $\mathcal{V}_z$  determined.

At this writing, this program has just begun and only preliminary data on radial oscillations has been obtained.

It is possible with this model to test systematically the effects of misalignments, errors in  $k$ , and other imperfections. It is also possible to attempt acceleration through resonances by altering  $k$  at a given radius. One program being considered is the radio frequency acceleration of the beam with a frequency modulated R.F. oscillator connected to the vacuum tank. With this system the problems of beam stacking of interest in opposed-beam accelerators might be studied. Also of interest might be the testing of various beam extraction techniques.

REFERENCES

Small Model FFAG Betatron, Terwilliger, Jones, Cole, Kerst, and Haxby, Phys. Rev. 100, 1246, (1955).

Design Parameters for an 8 Sector F.F.A.G. Mark Ib Model, Cole, Haxby, Jones, Kerst, and Terwilliger, MURA-FTC/ROH/LWJ/DWK/KMT - 1 (unpublished).

Detailed Calculations of a Small Model FFAG Mark Ib Accelerator, F. T. Cole and D. W. Kerst - MURA - FTC/DWK - 1 (unpublished) MURA - FTC - 2 (unpublished).

Equilibrium Orbit in Mark I FFAG, F. T. Cole, MURA/FTC - 4 (unpublished).

Determination of Sigma in the Model FFAG Mark Ib Accelerator, A. M. Sessler, MURA - AMS - 1 (unpublished).

Injection into the Mark Ib FFAG Model, L. W. Jones, MURA - LWJ - 10 (unpublished).

A Note on the Accelerated Beam Obtained in the Michigan Radial Sector F.F.A.G. Electron Model, L. W. Jones and K. M. Terwilliger, MURA - LWJ/KMT - 4 (unpublished)

Betatron Oscillations in the Synchrotron, C. L. Hammer, R. W. Pidd, and K. M. Terwilliger, Review of Scientific Instruments 26, 555, (1955).

FIGURE CAPTIONS

Figure 1 : Geometry of magnets and vacuum tank.

Figure 2 : Cross section drawing of a magnet.

Figure 3 : Photographs of a magnet showing detail of a coil card.

Figure 4a : The accelerator with field magnets and betatron core in position around the vacuum tank.

Figure 4b : The target probe region of the tank with one magnet removed showing the insulated flange joint between the two halves of the vacuum tank.

Figure 5 : Overall view of the accelerator room.

Figure 6 : Schematic Diagram of the two sector sigma test.

Figure 7 : Results of sigma test; values of  $\nu_x$  and  $\nu_z$  are given as a function of current ratios.

Figure 8 : Electron kinetic energy and magnetic field as a function of radius.

Figure 9 : Resonance diagram for this model with regions where accelerated beam is observed indicated. The region scanned by k- and current ratio - tuning is indicated.

# F.F.A.G. MODEL

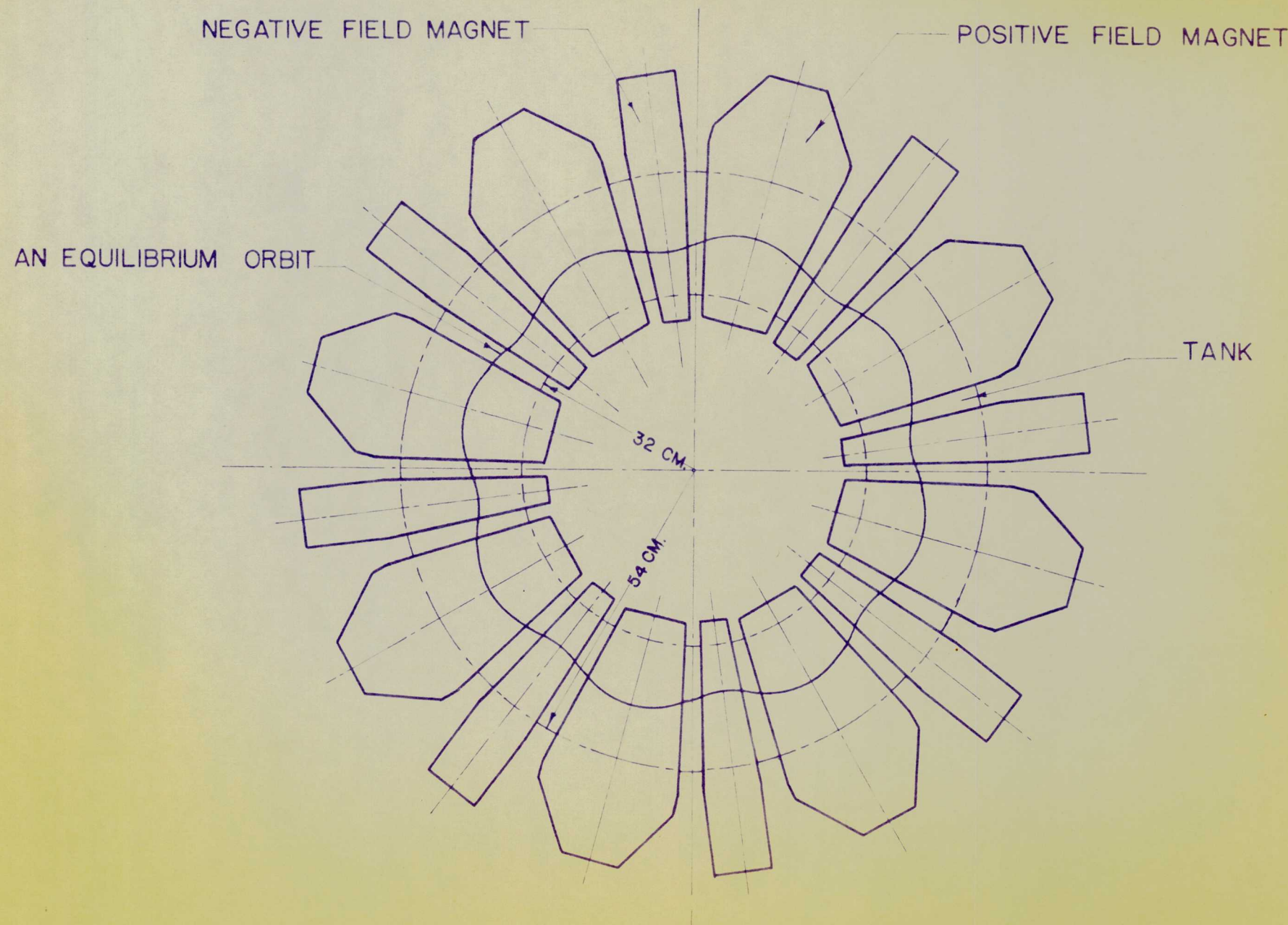


FIG. I - MAGNET LAYOUT WITH AN EQUILIBRIUM ORBIT

## F.F.A.G. MODEL

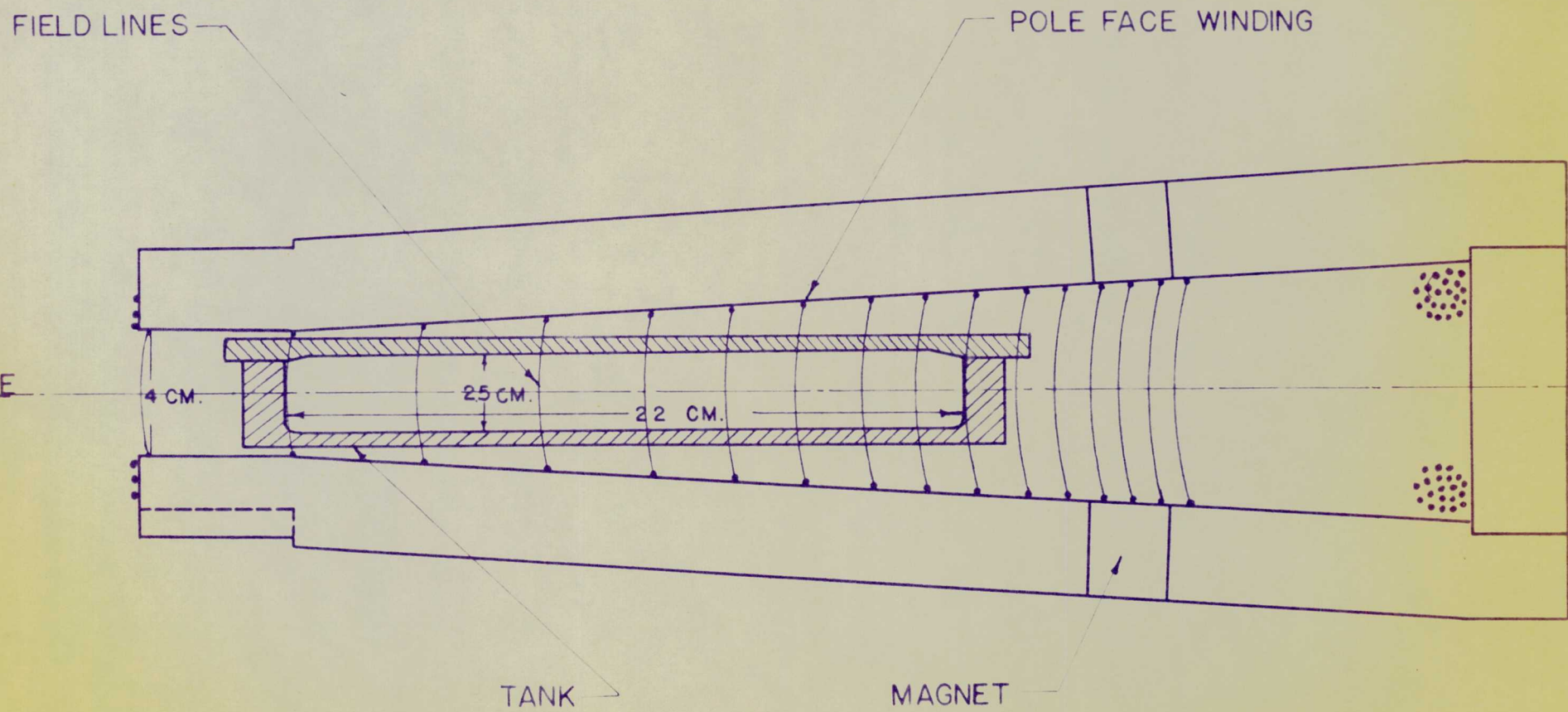


FIG.2

CROSS SECTION OF MAGNET AND TANK

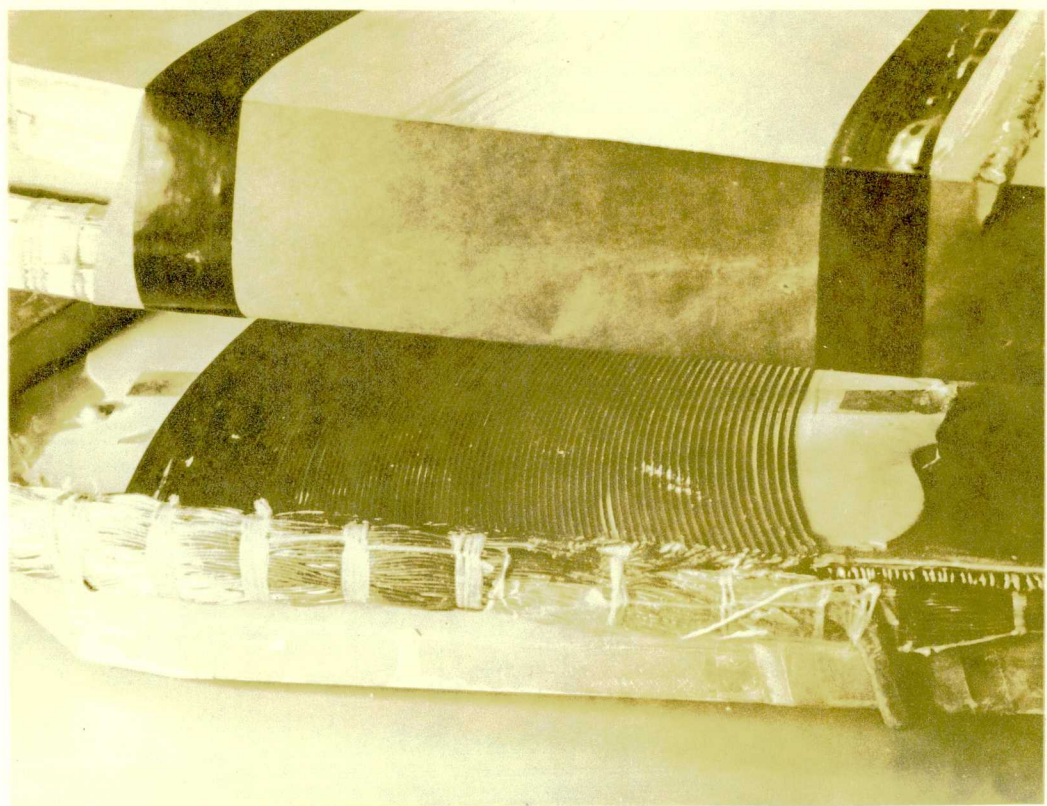
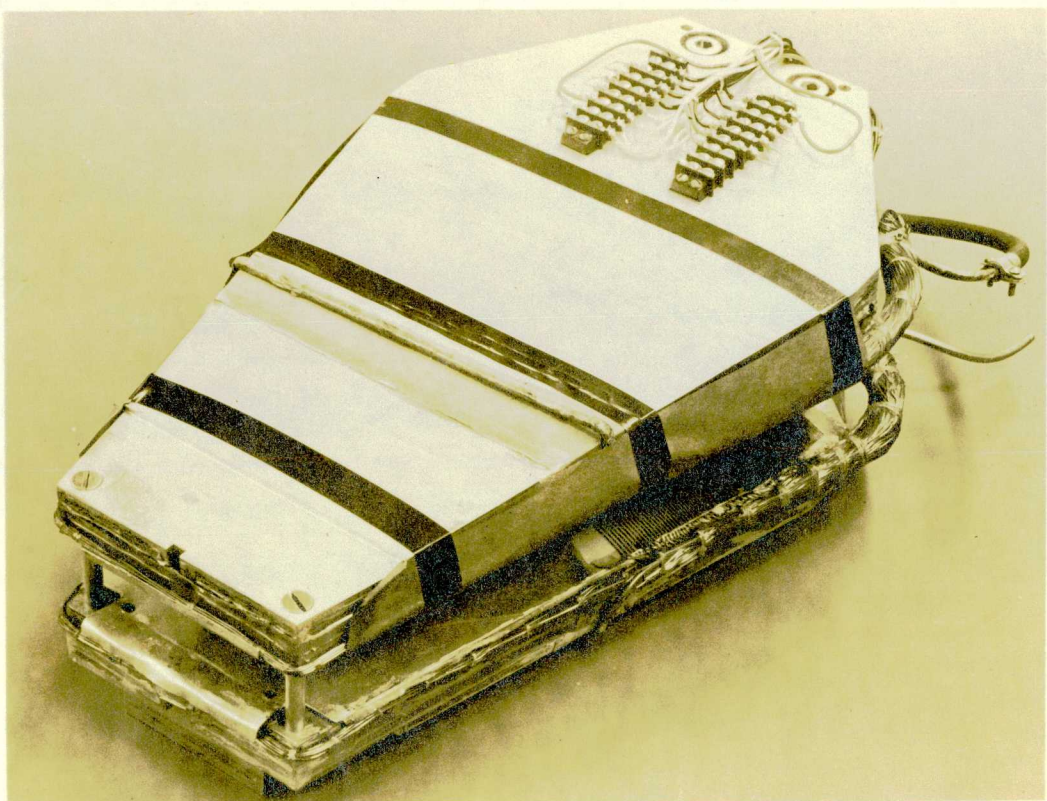


FIGURE 3

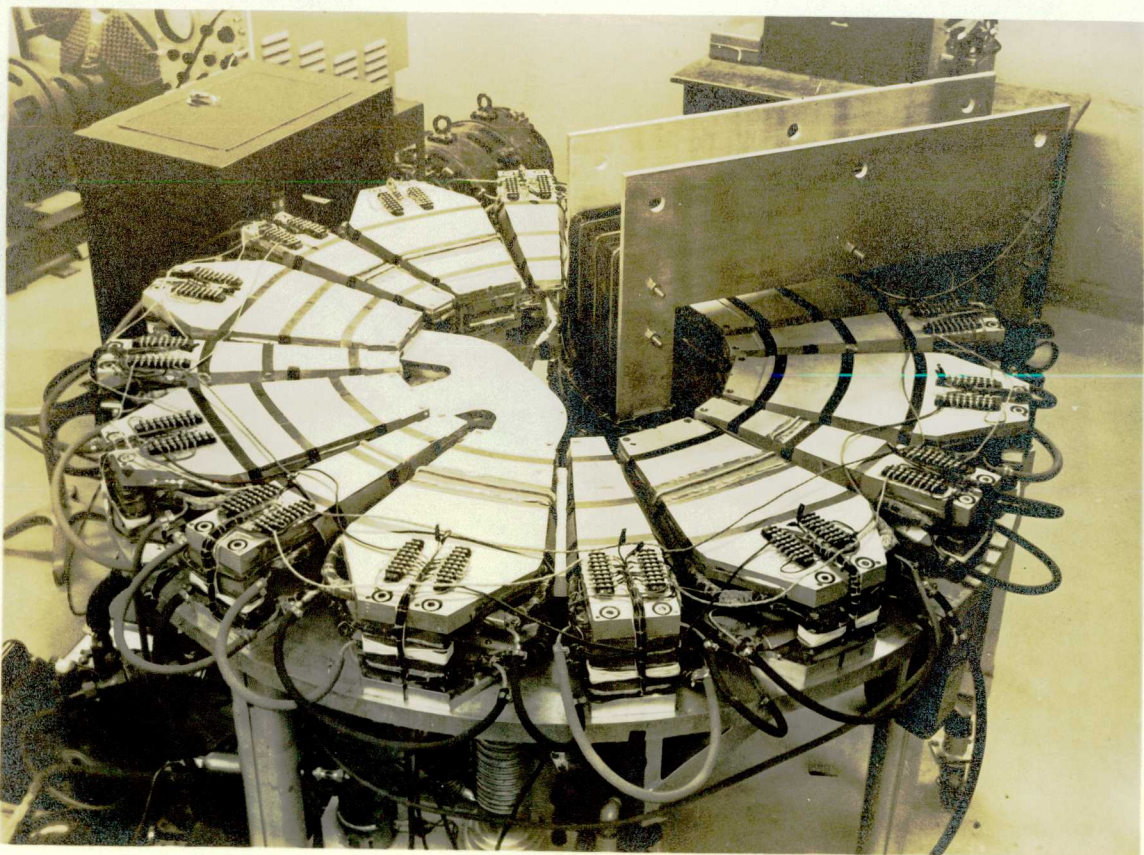
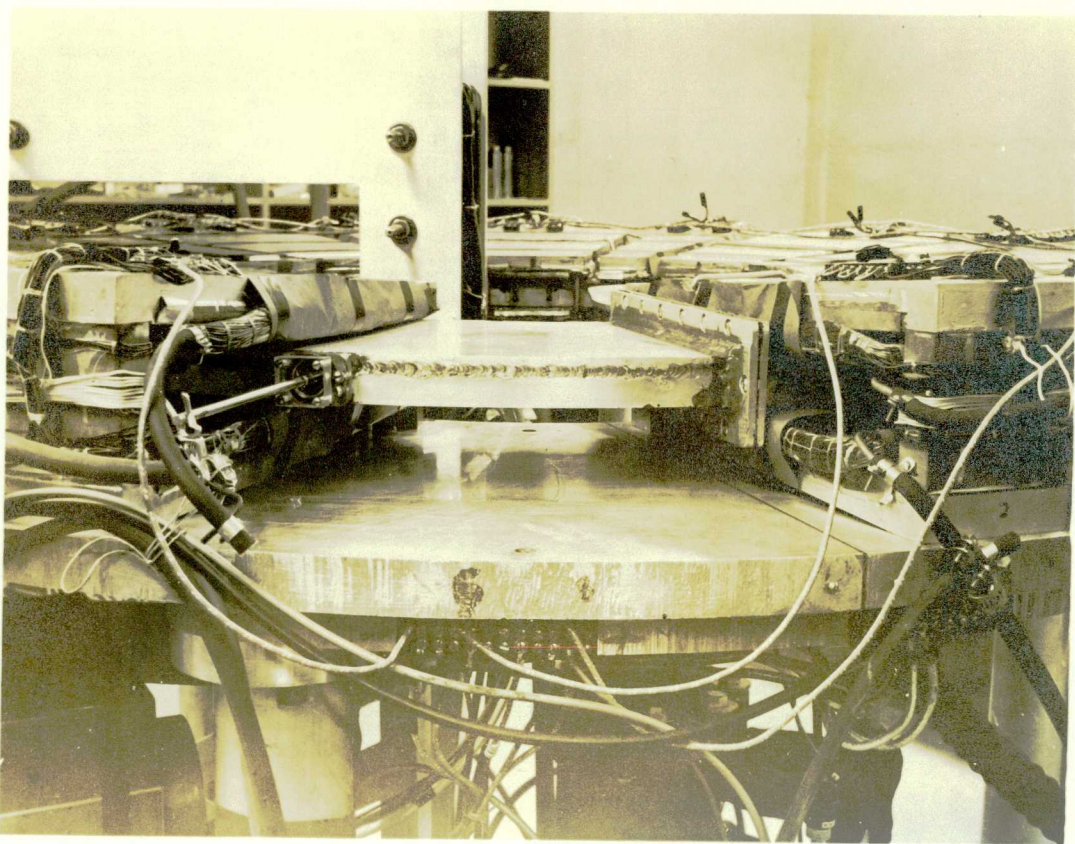


FIGURE 4a



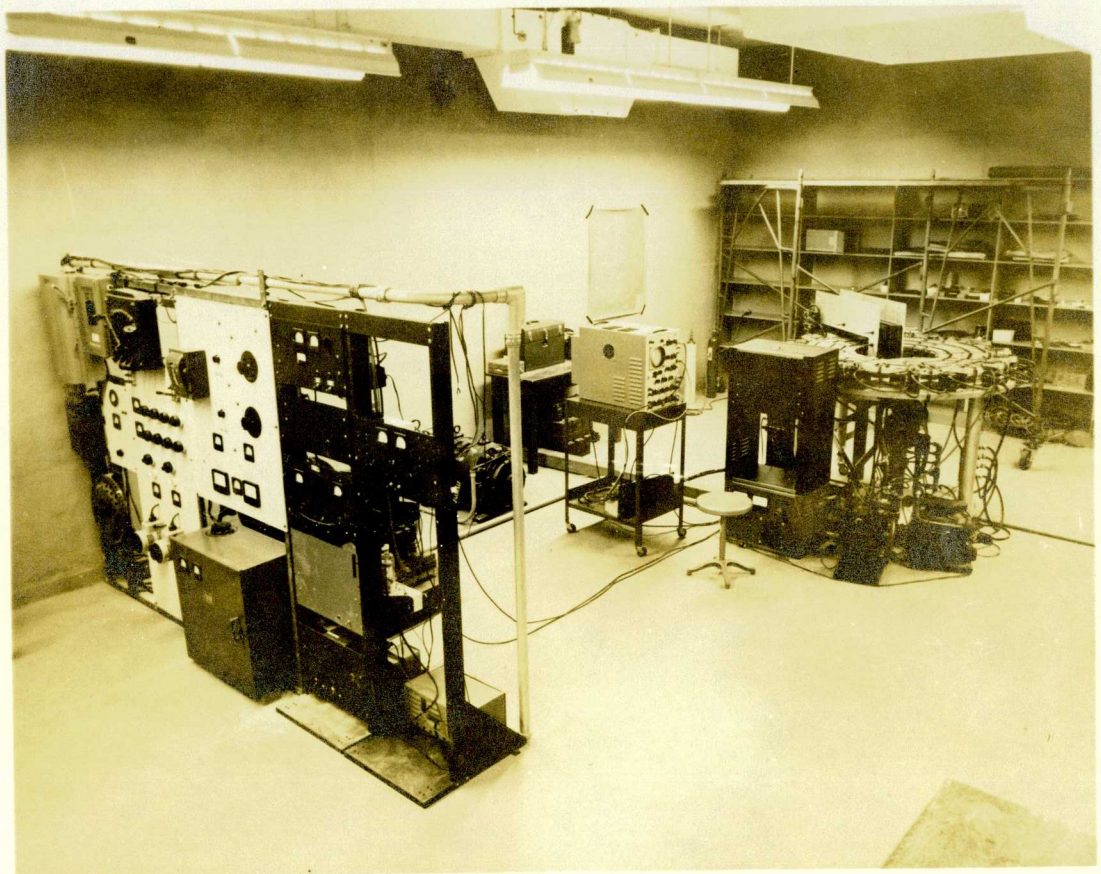
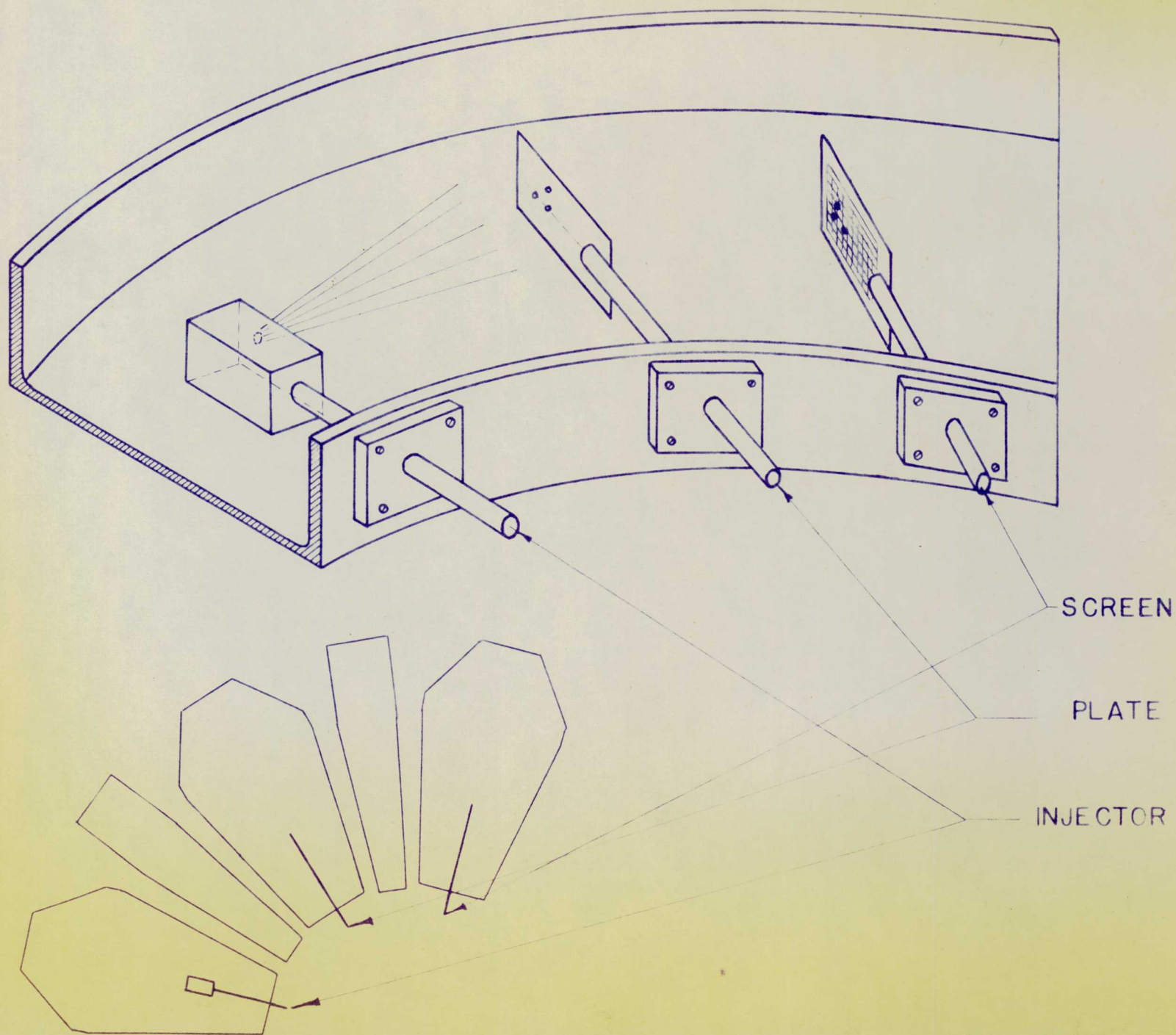
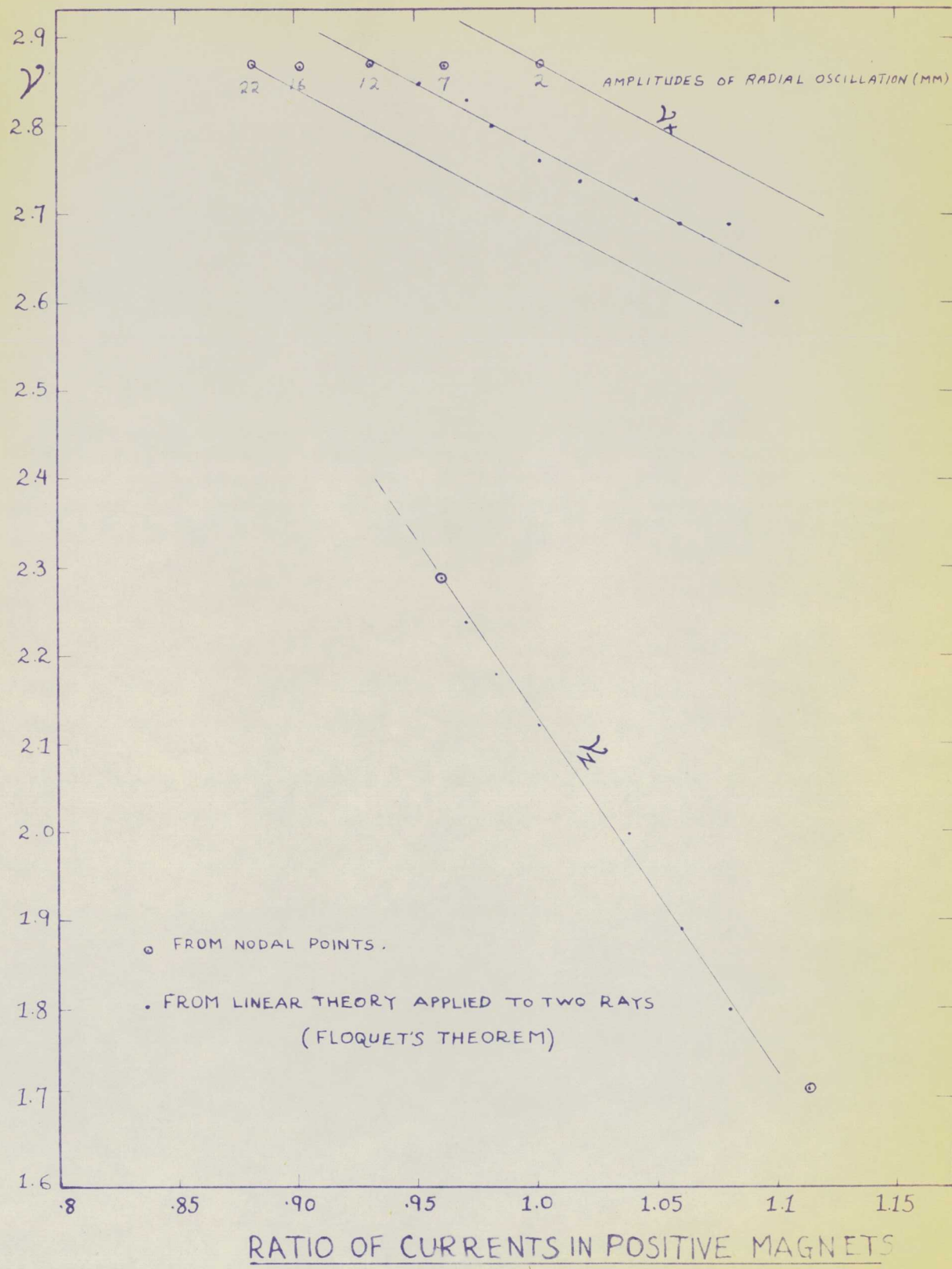


FIGURE 5

FIG.6- SCHEMATIC DIAGRAM OF SIGMA TESTING



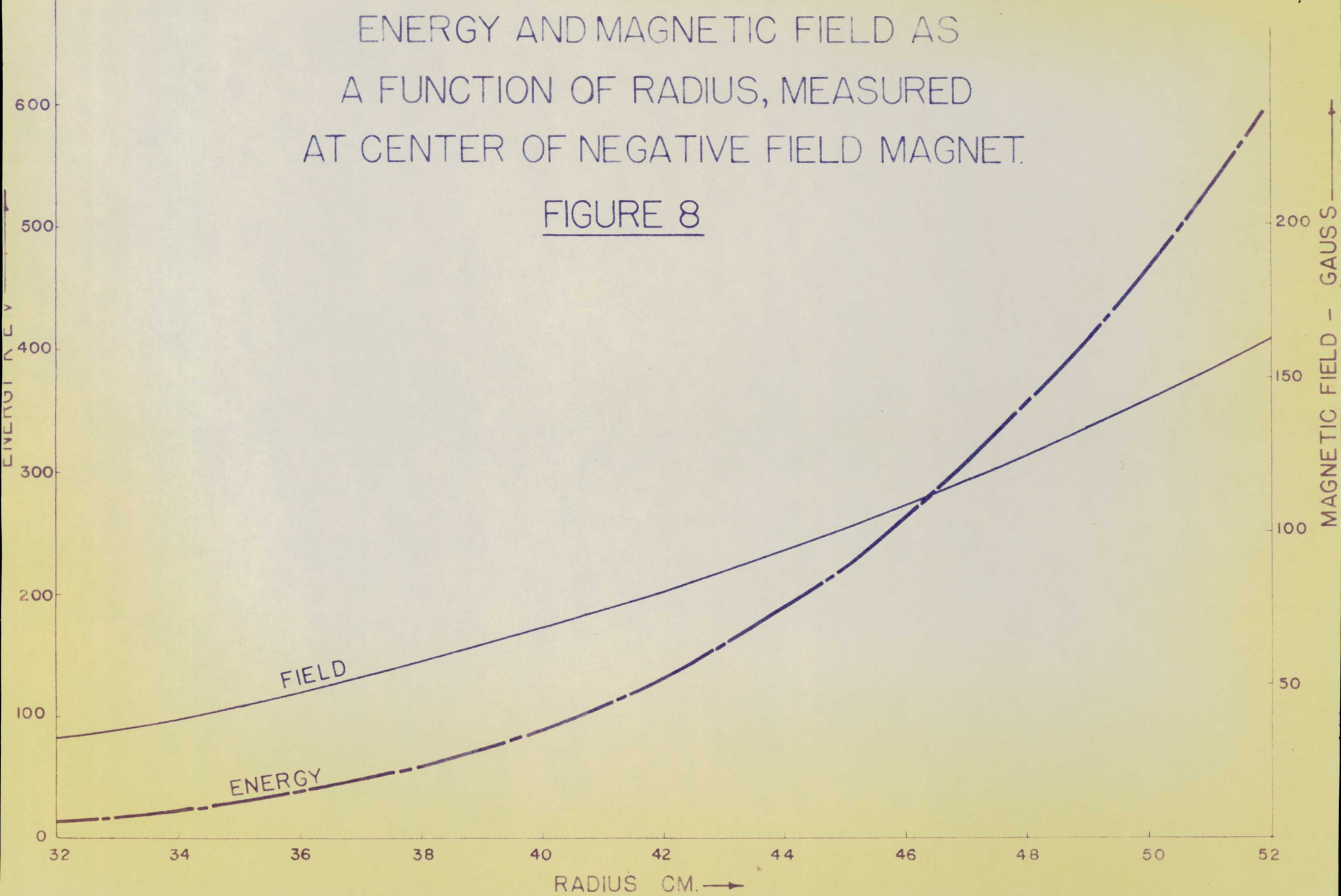


(FIG. 7)

## F.F.A.G. MODEL

ENERGY AND MAGNETIC FIELD AS  
A FUNCTION OF RADIUS, MEASURED  
AT CENTER OF NEGATIVE FIELD MAGNET.

FIGURE 8



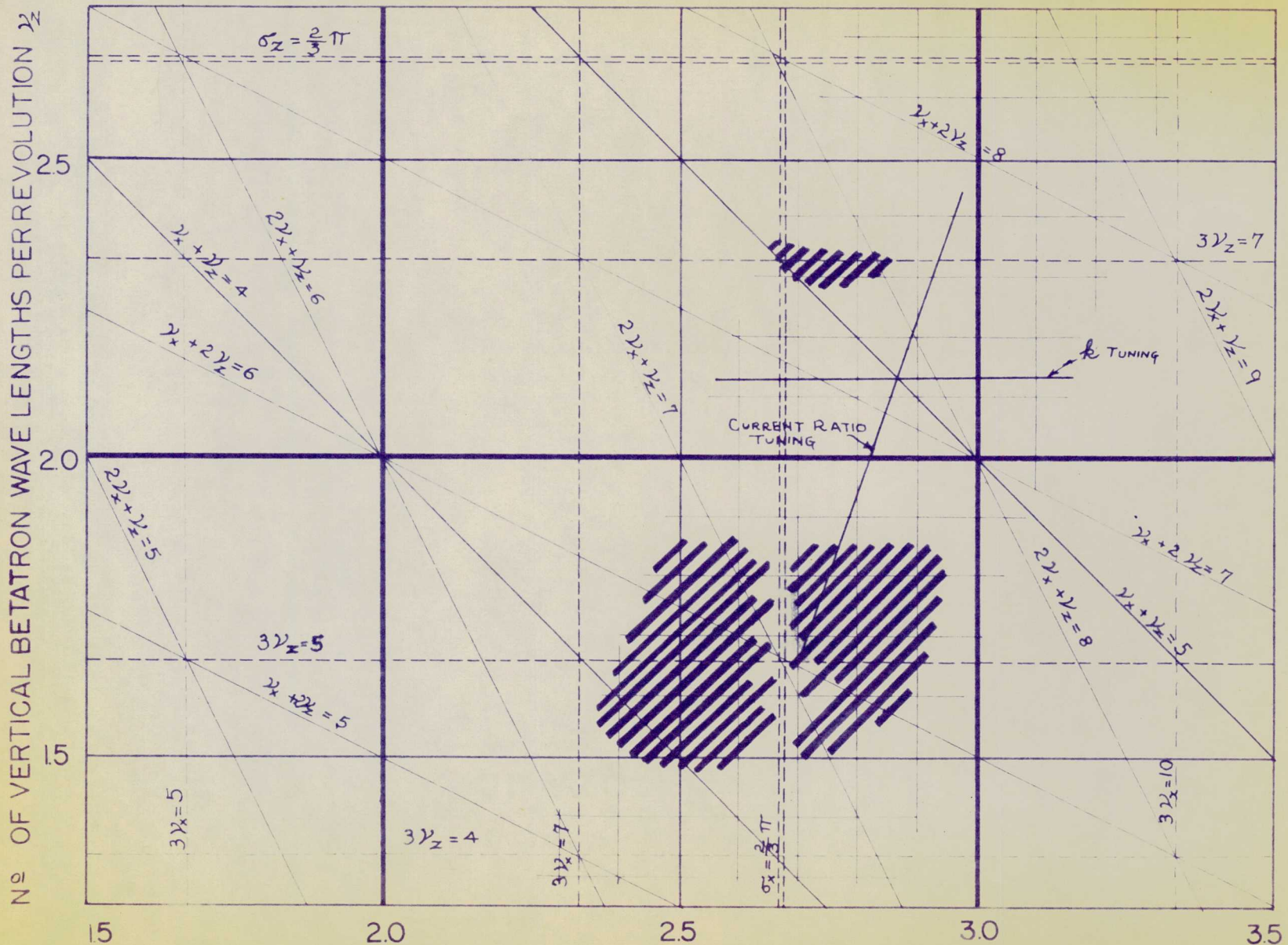


FIG 9 - NUMBER OF RADIAL BETATRON WAVE LENGTHS PER REVOLUTION  $2x$



REGION SCANNED BY TUNING



REGION WHERE ACCELERATED BEAM OBSERVED